Volume XI Issue 2 Year 2026 | Page 684-694| ISSN: 2527-9866
Received: ***20-05-2026*** | *Revised:* ***28-05-2026*** | *Accepted:* ***30-05-2026***

Convolutional Block Attention Module Integration into YOLO11 Architecture for MRI Image-based Brain Tumor Detection

Jendraja Husin Kotan[1], Yohannes[2], Hafiz Irsyad[3]
[1,2,3]Department of Informatics, Faculty of Computer Sciences and Engineering, Universitas Multi Data Palembang, Palembang, Sumatera Selatan, Indonesia, 30125
e-mail: jendrajahk0303@gmail.com[1], yohannesmasterous@mdp.ac.id[2], hafizirsyad@mdp.ac.id[3]
*Correspondence: jendrajahk0303@gmail.com

Abstract: *Brain tumor is one of the deadly diseases in the world that can affect anyone, this disease is characterized by the growth of abnormal cells or tissues in the brain, medically it can be life-threatening if not treated properly. Most tumor detection tasks are done by manual assessment by radiologists or pathologists where this work is time-consuming, so accurate and reliable detection is needed in the medical field in diagnosing brain tumors. The purpose of this study is to integrate CBAM on the YOLO11 architecture in detecting brain tumors and determine the performance of the brain tumor detection model using the YOLO11 architecture with CBAM integration. The method used to detect brain tumors is the YOLO11 architecture with CBAM integration. The dataset used is an image in the form of brain MRI. The results of this study indicate that the precision is 86.9%, recall is 86.2%, mAP50 is 91%, and mAP50-95 is 64% in the validation data and precision is 89.1%, recall is 92%, mAP50 is 79%, mAP50-95 is 51.6%, and F1 score is 90.5% in the test data which can be used to help medical personnel in detecting and treating brain tumors considering that this model has outstanding results, especially in the recall metric section which reaches 92% in the test data.*

Keywords: *Brain, CBAM, Detection, Tumor, YOLO11*

1. Introduction

Brain tumors are one of the world's deadliest diseases that can affect anyone. This disease, characterized by the growth of abnormal cells or tissue in the brain, can be medically life-threatening if not treated properly. [1] In general, brain tumors are classified into two main categories, benign and malignant. [2] In Indonesia, deaths from brain tumors rank after kidney disease, diabetes, stroke, and hypertension. Brain tumors affect approximately 300 patients annually in Indonesia, ranging from children to adults. According to the Indonesian Ministry of Health, epidemiological data collection on brain tumors in Indonesia is still lacking because it is not yet mandatory. Furthermore, brain tumor registration is often limited to malignant brain tumors, while benign brain tumors are often overlooked [3]. Frequent brain tumors generally require medical services with a basic understanding of diagnosis and treatment. Diagnosis is carried out by experts to patients through several methods, one of which is through medical imaging Magnetic Resonance Imaging (MRI) [4], which is a medical imaging technique that uses magnetic fields and radio waves to produce detailed two- or three-dimensional images of internal human organs and tissues [1]. MRI imaging can display the anatomical structure of the brain and can help experts detect tumors. Most tumor detection tasks are carried out by manual assessment by radiologists or pathologists, which is time-consuming, so accurate and reliable detection is needed in the medical field in diagnosing brain tumors. [4]

With the advancement of deep learning technology, Convolutional Neural Network (CNN)-based models have demonstrated remarkable capabilities in object detection and classification across various domains, including medical. One popular and efficient architecture for object detection,

especially in real-time, is You Only Look Once (YOLO), which is a deep learning algorithm designed for object detection using intelligent neural networks, and is also one of the deep learning models designed for real-time object detection. YOLO is known for its efficient ability to detect objects in images at high speed, without sacrificing accuracy. [5] YOLO has revolutionized industrial inspection processes by enabling faster, more accurate, and more cost-effective detection. In this context, YOLO11 represents one of the most advanced and efficient models, combining high inference speed with exceptional accuracy, making it an ideal choice for detection and classification applications. [6] YOLO11 is the latest development in the YOLO series, renowned for its efficient and powerful performance in real-time computer vision tasks. [7] YOLO11x has the highest mAP50 value compared to YOLO11l, YOLO11m, YOLO11s, YOLO11n, YOLOv8x, YOLOv8l, YOLOv8m, YOLOv8s, and YOLOv8n with the highest value obtained from YOLO11x at 54.7%. [8][9][10] This makes YOLO11 well-suited for applications requiring real-time analysis, where timely and accurate object recognition is crucial. Improvements in YOLO11 underscore its adaptability and potential in addressing diverse vision-based challenges [7]. MRI is one of the most effective imaging modalities for detecting brain abnormalities, including tumors. Unlike other imaging techniques such as CT scans, MRI does not use ionizing radiation, making it considered safer for long-term diagnosis. Manual analysis of MRI images by medical personnel is often time-consuming and prone to subjective errors, making the development of an Artificial Intelligence (AI)-based system crucial. [5]

Several previous studies have been conducted to detect brain tumors, for example using YOLOv7, where the results showed that the mAP obtained was 86%-93.2%, precision was 84.6%-91.8%, recall was 81%-90.2%, and F1 score was 82.5%-90.8% [4]. In addition, there was a previous study using YOLOv8 and SAM for brain tumor detection and segmentation, where the results showed that the mAP50 obtained was 89%, mAP50-95 was 70%, precision was 86%, and recall was 87% [11]. In addition, there is also a previous study that used YOLOv10 to detect brain tumors where the results showed that the precision obtained was 97.88%, recall was 95.24%, and mAP50 was 95.84% [5]. There is also a previous study that used YOLO11 to detect brain tumors where the results showed that the precision obtained was 95.6%, recall was 94.6%, mAP50 was 97.7%, and mAP50-95 was 80.9% [12].

YOLO has gained popularity due to its real-time detection and high accuracy, but its performance degrades on images due to various challenges. To address these limitations, attention mechanisms, specifically CBAM, which is designed to improve the sensitivity of convolutional neural network (CNN) features by focusing on the most informative parts of an image, have been introduced to improve feature representation by sequentially applying channel and spatial attention. Integrating CBAM into a detection framework can improve accuracy and robustness by allowing the model to focus on important features while suppressing background noise, which can then address unique detection challenges. This approach leverages the strengths of YOLO11, such as its detection capabilities and efficient architecture, while integrating CBAM to improve feature representation and handle complex backgrounds [7][13], so research is needed that aims to integrate CBAM in the YOLO11 architecture in detecting brain tumors.

2. Methods

A. Data Description

In this research, the data are carried out in the form of a public brain MRI image dataset obtained from [14]. The dataset used here is the 2024 version and has 3064 T1-weighted contrast-weighted images from 233 patients with three types of brain tumors: meningioma (708 images), glioma (1426 images), and pituitary (930 images).

B. Research Methodology

This section describes the steps taken in this research, from literature review to model testing. This research integrates the CBAM module into the YOLO11 architecture to detect brain tumors based on MRI image datasets.

1. Dataset Collection

At this stage, the dataset collection process is carried out in the form of a public brain MRI image dataset obtained from [14]. The dataset used here is the 2024 version and has 3064 T1-weighted contrast-weighted images from 233 patients with three types of brain tumors: meningioma (708 images), glioma (1426 images), and pituitary (930 images). Examples of a brain tumor MRI image dataset can be seen in Table 1.

Table 1. Example of Brain MRI Image Dataset

Image	Class	Label	Type of Tumor	Number of Image
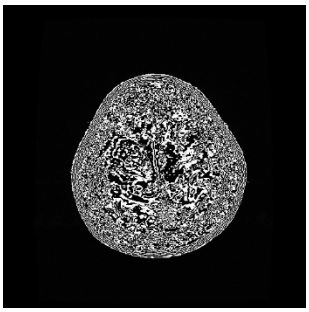	0	2	Glioma	1426
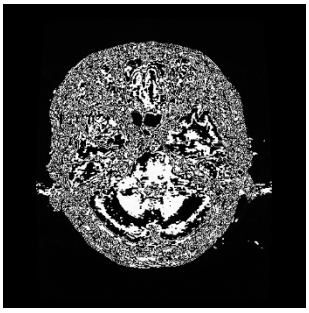	1	1	Meningioma	708
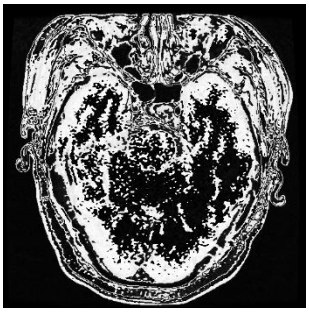	2	3	Pituitary	930

In the brain tumor dataset, there are five fields: label, PID, image, tumorBorder, and tumorMask. Label is an ID that specifies the type of tumor, with 1 being meningioma, 2 being glioma, and 3 being pituitary. PID is the patient ID. Image is the brain MRI image. tumorBorder is a vector that stores the coordinates of discrete points on the tumor boundary. For example, in [x1,y1,x2,y2,...], (xi,yi) are the planar coordinates of the tumor boundary. These vectors are generated by manually drawing the tumor boundary and can be used to generate a binary image called tumorMask, which

is a binary image with the number 1 indicating the tumor region. Of the total 3064 datasets in the form of brain tumor images, the dataset was divided into 70% training dataset, namely 2145, 20% validation dataset, namely 613, and 10% testing dataset, namely 306.

2. Design

At this stage, the required system design is carried out. The brain tumor detection process begins with receiving input in the form of a brain MRI image that is still in the .mat extension containing image data (grayscale image of brain tissue intensity), tumor mask (manual tumor segmentation as ground truth), and label (tumor type code, namely 1 is meningioma, 2 is glioma, and 3 is pituitary), then converted into .png format, then the system automatically divides the dataset into a training dataset (70%), a validation dataset (20%), and a testing dataset (10%). After the dataset division, the system will automatically download yolo11x.pt from GitHub and then inject CBAM into YOLO11. After that, the system will train on 70% of the training dataset first for 100 epochs and 8 batches, then continue with validation on 20% of the validation dataset, and finally continue with testing on 10% of the testing dataset.

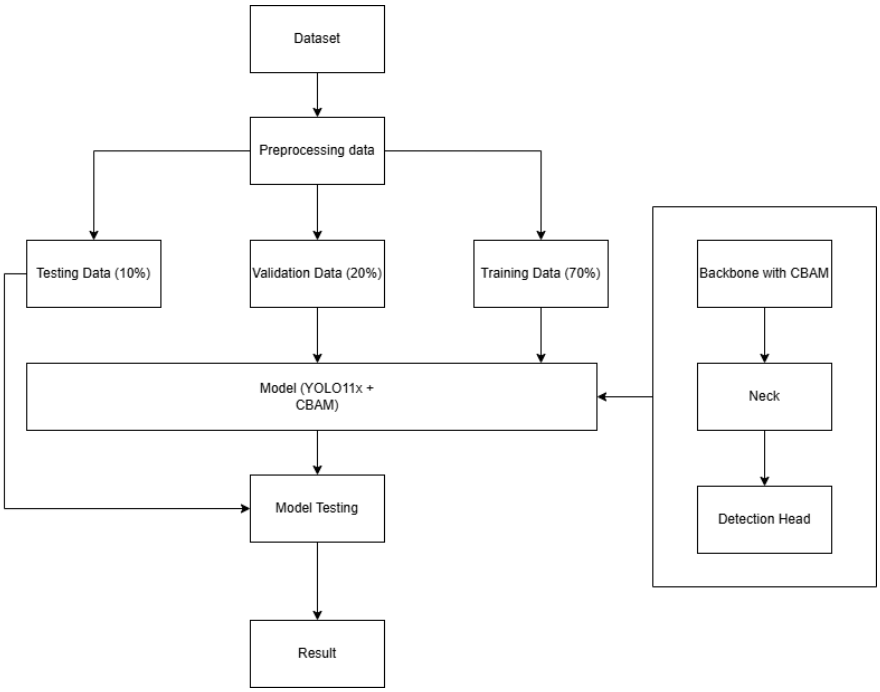

Figure 1. Diagram of Model Design

3. Implementation

At this stage, the previously designed model is implemented so that the model can recognize and detect the location of brain tumors based on previously processed MRI brain images.

4. Testing

At this stage, the previously created model will be tested on test data to see whether the previously created model meets expectations. After the trial phase, the test results are calculated to obtain the success rate of the method used with the confusion matrix in calculating the precision, recall, F1 score, and mAP values. Precision measures how accurate the model's positive predictions are by comparing the number of true positives to the total number of positive predictions, including false positives, while recall compares the number of true positives to the number of true positives and false negatives. The F1 score combines precision and recall into a single value by calculating the harmonic mean of both. This metric provides a more balanced assessment of model performance because it considers both false positives and false negatives [15]. mAP is the post-testing accuracy value specifically used by the YOLO architecture.

3. Results and Discussion

This section presents the research results, including the integration of the CBAM module into the YOLO11 architecture for brain tumor detection. Each stage of the system, from dataset preparation to the final results, is explained in detail based on the system design diagram.

A. Model Architecture

The model used in this study is YOLO11x, the largest variant of the YOLO11 model family, with a total of 56,966,176 parameters and a computational capacity of 195.5 GFLOPs. This model uses pretrained weights from the COCO dataset to leverage transfer learning capabilities. To improve the model's ability to focus attention on spatially and channel-relevant features, a CBAM module was injected into the YOLO11x backbone architecture. The CBAM module was successfully injected into four network layers. The integration of CBAM into YOLO11 is expected to improve detection accuracy, particularly for classes with high visual variation, such as gliomas.

B. Training Configuration

The training process was carried out using an NVIDIA A100-SXM4-40GB GPU accelerator with a memory capacity of 40,441 MiB. The configurations used in the training are summarized in Table 2.

Table 2. Training Configuration

Parameter	Value
Number of Epoch	100
Batch Size	8
Input Image Size	$640\ px \times 640\ px$
Optimizer	AdamW
Initial Learning Rate	0.001
Final Learning Rate	0.01
Momentum	0.937
Weight Decay	0.0005
Warmup Epochs	3
Patience (early stopping)	15
Automatic Mixed Precision (AMP)	Active

Data augmentation was applied during training to improve the model's generalization capabilities, including a random horizontal flip with a probability of 0.5, changes in HSV values (hue, saturation, value), and albumentations-based augmentations including blur, median blur, grayscale conversion, and CLAHE (Contrast Limited Adaptive Histogram Equalization). In addition, the mosaic augmentation technique was also applied up to 10 epochs before the last epoch, then disabled in the final 10 epochs to help stabilize model convergence.

C. Training Result

The YOLO11x model training process with CBAM injection lasted for 97 epochs with a total duration of 1.635 hours (approximately 98.1 minutes), before being stopped by the early stopping mechanism due to no improvement in validation metrics for 15 consecutive epochs after the best epoch at epoch 82, where precision reached 86.7%, recall reached 86.3%, mAP50 reached 91.1%, and mAP50-95 reached 64%.

D. Validation Result

After the training process was completed, the best model saved at epoch 82 was thoroughly evaluated on the validation data using the Ultralytics framework. The results of the evaluation of the best model on the validation data are presented in Table 3.

Table 3. Best Model Validation Results

Class	Precision	Recall	mAP50	mAP50-95
All	86.9%	86.2%	91%	64%
Meningioma	94.8%	95.8%	98.7%	80.5%
Pituitary	91.7%	91.1%	95.6%	63.5%
Glioma	74.1%	71.7%	78.7%	48%

Overall, the best model yielded an mAP50 of 91% and an mAP50-95 of 64% on the validation data. Lower mAP50-95 values compared to mAP50 are common in object detection tasks, as these metrics evaluate the localization accuracy of the detection box at various IoU thresholds (from 0.5 to 0.95) and thus provide a more stringent assessment. At the class level, the meningioma class achieved the highest performance with an mAP50 of 98.7% and a recall of 95.8%, indicating that the model is highly reliable in detecting this type of tumor. The pituitary class also performed very well with an mAP50 of 95.6% and a precision of 91.7%. Conversely, the glioma class performed the lowest among the three classes with an mAP50 of 78.7% and a recall of only 71.7%, indicating that the model missed glioma detection more often than the other two classes. This difference in performance is likely due to the more heterogeneous morphological characteristics of gliomas and the ill-defined tumor margins on MRI images.

E. Testing Results

Comprehensive testing was conducted on 306 test data images completely separate from the data used in the training and validation processes. The testing used a confidence threshold of 0.25 and an IoU threshold of 0.45. The total time required to process the entire test data was 6 minutes and 9 seconds. The test results on all test data are presented in Table 4.

Table 4. Model Testing Results on Test Data

Metric	Value
mAP50	79%
mAP50-95	51.6%
Precision	89.1%
Recall	92%
F1 Score	90.5%
IoU Mean	81.9%
TP	253
FP	31
FN	22

The model successfully achieved an F1 score of 90.5%, reflecting an outstanding balance between precision and recall across the entire test data. The Mean IoU value of 0.8188 indicates that the model's detection boxes have a high average overlap with the ground truth, indicating accurate localization capabilities. Of the 306 tested images, the model successfully detected 253TP, with 31 FP and 22 FN. Evaluation of each class on the test data resulted in varying performance between classes as presented in Table 5.

Table 5. Model Test Results for each Class on Test Data

Class	Precision	Recall	mAP50	mAP50-95	F1 Score	TP	FP	FN	GT
Meningioma	96.7%	98.3%	85.5%	68.5%	97.5%	59	2	1	69
Pituitary	91.6%	96.2%	89.5%	58.8%	93.8%	76	7	3	83
Glioma	87.4%	87.1%	69.4%	38.9%	87.1%	118	17	18	154

The meningioma class performed best with a recall of 98.3% and an F1 score of 97.5%, meaning the model successfully detected 69 meningioma samples in the test data with one missed sample (FN = 1), and there were 2 false detections (FP = 2). The pituitary class also achieved very high performance with an F1 score of 93.8%, where only 3 samples were not detected out of a total of 83 ground truth samples. On the other hand, the glioma class had the lowest performance compared to the other two classes, with an mAP50 of 69.4% and there were 18 undetected cases (FN = 18) out of a total of 154 ground truth samples. However, the glioma F1 score of 87.1% is still considered good, indicating that the model is still able to optimally detect most glioma cases.

F. Detection Visualization

The system generates a structured visualization in the form of a 3×3 grid showing one representative sample per combination of phases (training, validation, and testing) and tumor class (glioma, meningioma, and pituitary). Each grid cell displays an MRI image with two layers of stacked annotation: a ground truth bounding box in white dashed lines as the original annotation reference, and a prediction bounding box in colored solid boxes (red for glioma, green for meningioma, blue for pituitary) as the model output. The label inside each prediction box lists the abbreviated class name, confidence score, and IoU value against the ground truth.

This grid visualization has significant diagnostic value. Samples from the training phase generally show outstanding agreement between ground truth and predictions, which can be attributed to the model's familiarity with the patterns it has "seen" during training. Samples from the validation and testing phases show greater variation: some show highly accurate predictions with an IoU above 0.85, others show bounding boxes that are slightly larger or smaller than ground truth but still correctly identify the area, and a small subset, particularly in the glioma class, show more substantial discrepancies due to diffuse tumor boundaries. In addition to the overview grid, the system generates three separate detailed visualization files for the training (Figure 3), validation (Figure 4), and testing (Figure 5) phases. Each file displays three samples per class (a total of 9 images per file in a 3×3 class×sample grid), providing a more comprehensive picture of the variability in the tumor's visual appearance and the model's response to that variability. Figure 2 presents a visualization of the results of brain tumor detection from the three classes, while Figure 3 presents a visualization of the results of brain tumor detection from the three classes during the training phase.

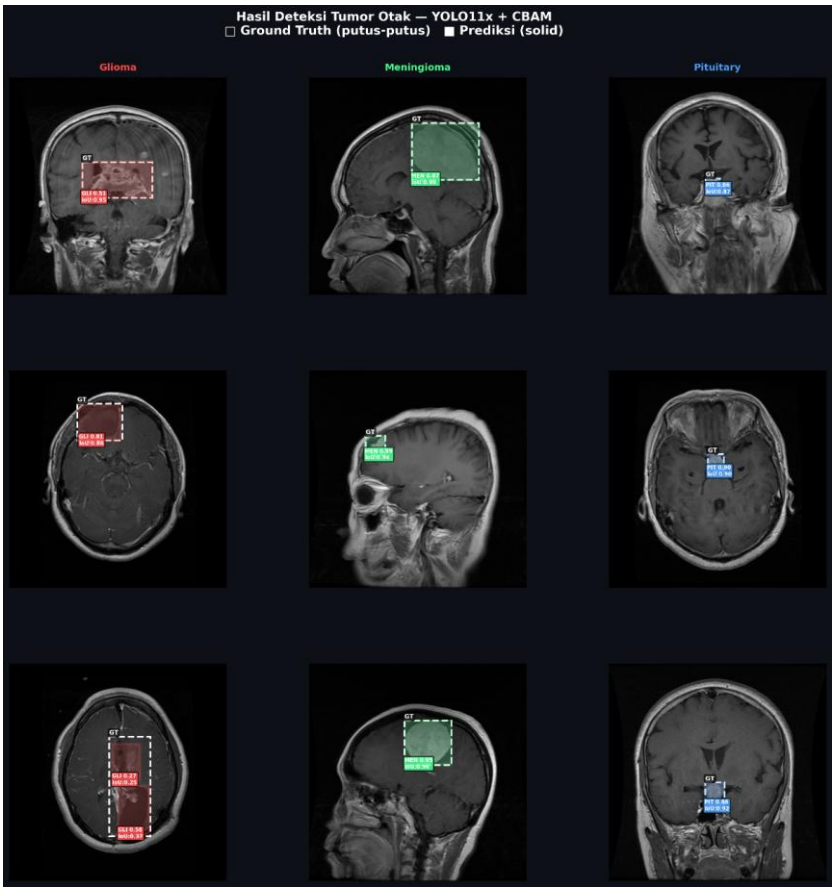

Figure 2. Visualization of Brain Tumor Detection Results

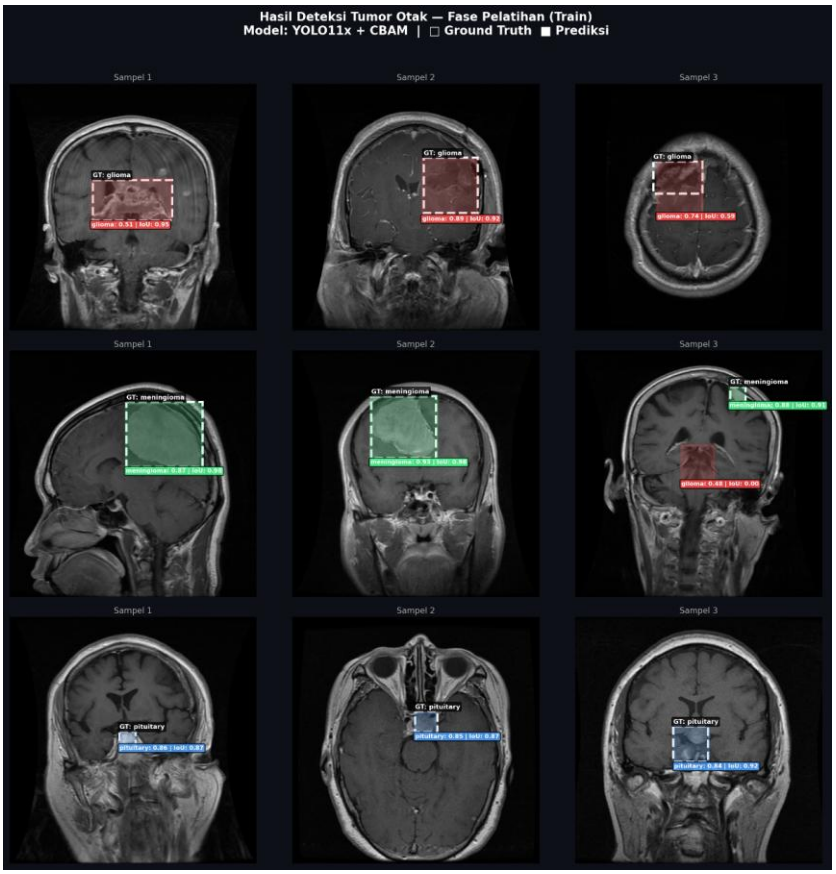

Figure 3. Visualization of Brain Tumor Detection Results of the Training Phase

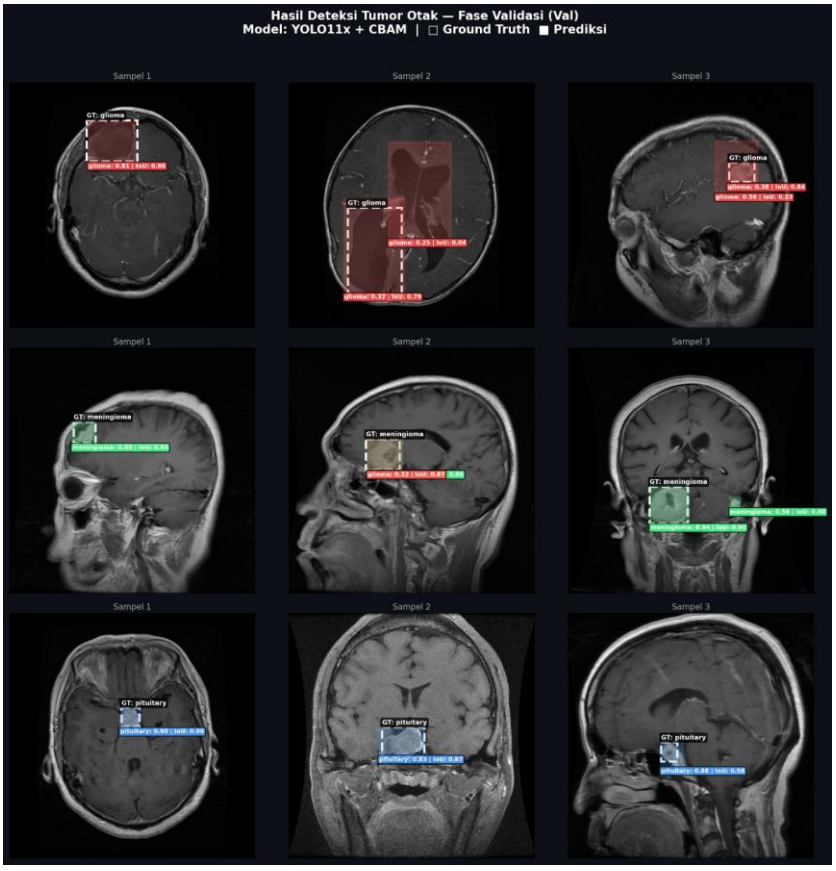

Figure 4. Visualization of Brain Tumor Detection Results of the Validation Phase

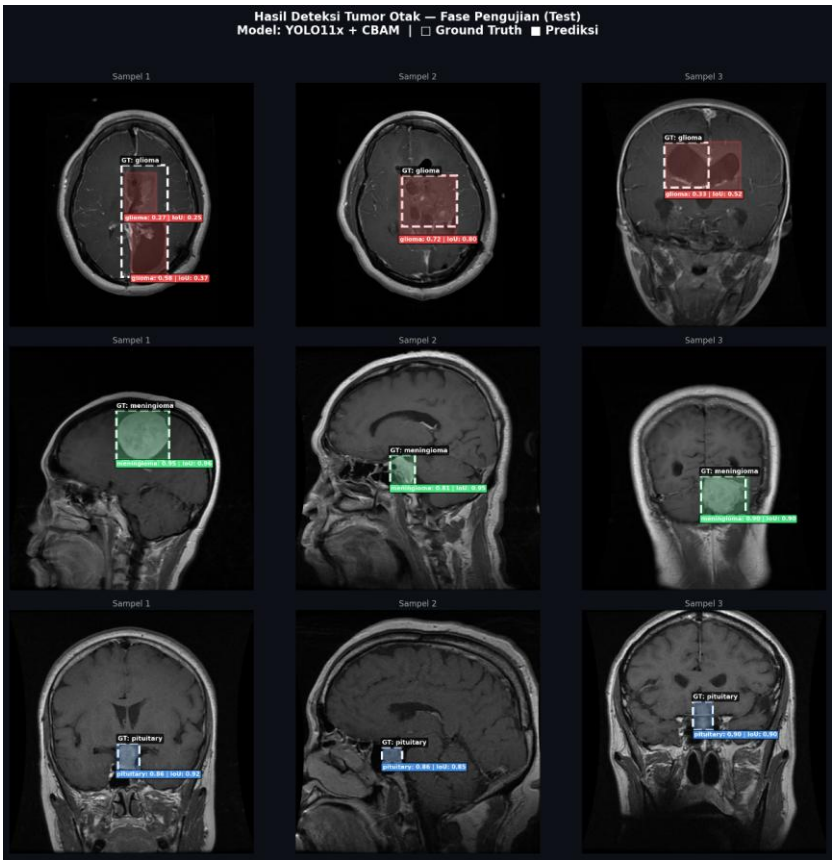

Figure 5. Visualization of Brain Tumor Detection Results of the Testing Phase

Figure 4 presents a visualization of the results of brain tumor detection from the three classes during the validation phase, while Figure 5 presents a visualization of the results of brain tumor detection from the three classes during the testing phase. A closer look at the detailed visualizations in the testing phase revealed several patterns consistent with the quantitative metric findings. In the meningioma class, all three samples consistently displayed predicted bounding boxes that nearly perfectly overlapped with the ground truth, with confidence scores ranging from 0.85–0.97 and an IoU above 0.82. In the pituitary class, predictions were generally accurate in identifying the sella turcica area, although the box dimensions sometimes slightly exceeded (or fell short of) the ground truth for small adenomas. In the glioma class, the greatest variation was observed, with some samples displaying outstanding predictions while others exhibited bounding boxes that were wider than the ground truth, reflecting the fundamental challenge of defining diffuse tumor boundaries.

4. Conclusions

This study successfully built and trained a brain tumor detection model based on the YOLO11x architecture injected with the CBAM module that achieved satisfactory performance on the three types of brain tumors studied. The model was successfully trained for 97 epochs with early stopping active at the 97th epoch, where the best model was obtained at the 82nd epoch with a precision of 86.7%, a recall of 86.3%, an mAP50 of 91.1%, and an mAP50-95 of 64%. The evaluation results on the validation data showed a precision of 86.9%, a recall of 86.2%, an mAP50 of 91%, and an mAP50-95 of 64% indicating competitive tumor localization capabilities. On a test dataset of 306 images, the model achieved 89.1% precision, 92% recall, 79% mAP50, 51.6% mAP50-95, 90.5% F1 score, and 81.9% average IoU. The 92% recall on the test dataset indicates that the model is capable of detecting most existing brain tumors, which is a critical aspect in medical applications to reduce the number of FNs. The 12% difference between the mAP50 values for the validation data (91%) and the mAP50 for the test data (79%) indicates mild to moderate

overfitting in the results of this study. This is likely due to the relatively small size of the test dataset (10% of the total), which makes the estimates unstable. Furthermore, YOLO11x was designed for large-scale datasets (>118,000 images), so the model has far more parameters than needed to learn the three tumor classes. Under these conditions, the model does not learn, but rather memorizes. CBAM injection exacerbates this situation by adding an additional representation dimension (channel attention + spatial attention), further increasing capacity without any additional constraints. In addition, glioma was already the weakest class even in the validation data. This means the model never truly mastered glioma during training, but instead only learned a limited version. This is due to the extreme morphological heterogeneity. Gliomas cover a wide spectrum from WHO Grade I to Grade IV (glioblastoma), each with a very different MRI appearance. Diffuse and infiltrative gliomas lack a clear boundary from the surrounding normal brain tissue, fundamentally different from meningiomas, which are almost always sharp-edged (extra-axial, well-circumscribed), and pituitaries, which are anatomically contained within the sella turcica, making their location highly predictable. Then, the CBAM mechanism consists of channel attention (selecting which feature maps are important) and spatial attention (selecting which spatial regions are important). For tumors with sharp edges, such as meningiomas, spatial attention works optimally, providing a contrasting and consistent local signal to pay attention to. For infiltrative gliomas, discriminatory features are diffusely distributed, often in the form of subtle signal heterogeneity over a large area. The CBAM mechanism consists of channel attention (selecting which feature maps are important) and spatial attention (selecting which spatial regions are important). For tumors with sharp edges, such as meningiomas, spatial attention works optimally, creating a contrasting and consistent local signal to observe. For infiltrative gliomas, discriminatory features are diffusely distributed, often in the form of subtle signal heterogeneity over a large area so CBAM spatial attention tends to focus on local signal peaks and ignores the peritumoral context that is actually important for defining glioma boundaries. Therefore, this model can be used to assist medical personnel in detecting and treating brain tumors, considering that this model has outstanding results, especially in the recall metric, which reaches 92% on test data. However, it is recommended to enlarge and balance the dataset because the uneven class distribution contributes to performance variations between classes, increase the proportion of the test set because the current test set is relatively small to estimate robust performance, strengthen regularization strategies such as increasing data augmentation, adding dropout to the head layer, and label smoothing to reduce the model's overconfidence in the training data so that overfitting is reduced to below 12%, and develop the model towards instance segmentation using YOLO11m with CBAM injection and YOLO11m-Seg so that tumor boundaries can be mapped more accurately. In addition, it is also recommended to use the latest versions of YOLO, namely YOLO26m and YOLO26m-Seg, so that the results of brain tumor detection in the form of bounding boxes on MRI images along with tumor boundaries can be mapped more accurately than the YOLO11 variant.

References

[1] D. Husen, “Klasifikasi Citra MRI Tumor Otak Menggunakan Metode Convolutional Neural Network,” *Bit-Tech (Binary Digital - Technology)*, vol. 7, no. 1, pp. 143–152, 2024, doi: 10.32877/bt.v7i1.1576.

[2] Yohannes, W. Widhiarso, and I. Pratama, “Combination of DWT Variants and GLCM as a Feature for Brain Tumor Classification,” in *2021 8th International Conference on Electrical Engineering, Computer Science and Informatics (EECSI)*, IEEE, Oct. 2021, pp. 197–202. doi: 10.23919/EECSI53397.2021.9624249.

[3] T. S. Sondakh, "Prevalensi dan Karakteristik Tumor Otak Primer di RSUP DR. Wahidin Sudirohusodo Tahun 2018-2023," Makassar, 2024.

[4] R. S. Passa *et al.*, "DETEKSI TUMOR OTAK PADA MAGNETIC RESONANCE IMAGING MENGGUNAKAN YOLOv7," *Jurnal Ilmiah MATRIK*, vol. 25, no. 2, pp. 116–121, 2023.

[5] A. I. Ahadin, F. M. Hana, and A. Prihandono, "Pengembangan Model Deteksi Tumor Otak pada Magnetic Resonance Imaging Menggunakan Arsitektur YOLOv10," *Sainteks*, vol. 21, no. 2, pp. 117–128, 2024, doi: 10.30595/sainteks.v21i2.23989.

[6] A. S. Khan, A. Rahman, and A. J. Moshayedi, "Pipeline Surface Defect Detection Using YOLOv11 with Attention Mechanisms: A Comparative Study of SA, LKA, and CBAM Approaches," *Journal of Robotics Research*, vol. 2, no. 2, pp. 1–9, 2025, doi: 10.64820/AEPJRR.22.1.9.122025.

[7] R. Sapkota and M. Karkee, "Integrating YOLO11 and Convolution Block Attention Module for Multi-Season Segmentation of Tree Trunks and Branches in Commercial Apple Orchards," 2024, [Online]. Available: http://arxiv.org/abs/2412.05728

[8] G. Jocher, "Explore Ultralytics YOLOv8 - Ultralytics YOLO Docs." Accessed: Oct. 30, 2025. [Online]. Available: https://docs.ultralytics.com/models/yolov8/

[9] G. Jocher, "Ultralytics YOLO11 - Ultralytics YOLO Docs." Accessed: Oct. 30, 2025. [Online]. Available: https://docs.ultralytics.com/models/yolo11/

[10] Y. Tian, Q. Ye, and D. Doermann, "YOLOv12: Attention-Centric Real-Time Object Detectors," 2025. [Online]. Available: http://arxiv.org/abs/2502.12524

[11] Ardiansyah, K. N. Qodri, D. Al Banna, and M. Z. Al Baihaqi, "Pemanfaatan SAM dan YOLOv8 untuk Deteksi dan Segmentasi pada Citra MRI Tumor Otak (Utilization of SAM and YOLOv8 to Detection and Segmentation of Brain Tumor on MRI Image)," *TEKNIMEDIA*, vol. 5, no. 1, pp. 82–89, 2024.

[12] Ardiansyah, A. S. Widagdo, K. N. Qodri, D. Hidayani, and M. Romadhani, "Implementasi Deteksi Tumor Otak Menggunakan YOLOv11 dan Flask," *JURNAL FASILKOM*, no. 2, pp. 415–422, 2025.

[13] N. Garshasebi, "Improving Small Object Detection in Remote Sensing with YOLO11-CBAM and Deep Learning," *Journal of China University of Geosciences*, vol. 50, pp. 217–227, 2025, doi: 10.5281/zenodo.15845503.

[14] J. Cheng, "Item - brain tumor dataset - figshare - Figshare." Accessed: Jan. 10, 2026. [Online]. Available: https://figshare.com/articles/dataset/brain_tumor_dataset/1512427/8

[15] L. P. Tappi and C. Dewi, "Klasifikasi Penyakit Kulit menggunakan YOLO11," *Jurnal Inovtek Polbeng - Seri Informatika*, vol. 10, no. 2, p. 2025, 2025.